Structure of 0^+ excitations in the mass $A \approx 100$ region: 0_2^+ bands in ^{98}Sr and ^{100}Zr

W. Urban,[1] T. Rząca-Urban,[1] J. Wiśniewski,[1] I. Ahmad,[2] A. G. Smith,[3] and G. S. Simpson[3]
[1]*Faculty of Physics, University of Warsaw, ulica Pasteura 5, PL-02-093 Warsaw, Poland*
[2]*Argonne National Laboratory, Argonne, Illinois 60439, USA*
[3]*Department of Physics and Astronomy, The University of Manchester, M13 9PL Manchester, United Kingdom*

(Received 23 January 2019; revised manuscript received 29 April 2019; published 21 June 2019)

0_2^+ bands in ^{98}Sr and ^{100}Zr, populated in spontaneous fission of ^{248}Cm and ^{252}Cf, have been studied using the Eurogam2 and Gammasphere arrays. Phenomenological classification of excited 0^+ levels in even-even nuclei of the $A \approx 100$ region into four categories is presented and an interpretation for each category is proposed. Highly deformed 0_1^+ ground states and low-energy 0_2^+ levels in both nuclei are probably due to the 2p-2h excitation of two neutrons from the $9/2^+[404]$ extruder to the low-Ω prolate and the $11/2^-[505]$ oblate orbitals originating from the $h_{11/2}$ shell, respectively. Candidates for 0^+, β vibrational states in $A \approx 100$ region are suggested at $N > 60$.

DOI: 10.1103/PhysRevC.99.064325

I. INTRODUCTION

Low-lying 0^+ excitations are often a sign of coexisting shapes [1], a phenomenon of prime importance for testing nuclear models. In spite of their fundamental role there are growing differences among interpretations of such levels. Many of them were reported as so-called β vibrations introduced by Bohr and Mottelson [2]. However, recent works put into question the existence of such excitations or, at least, significantly limit their occurrence [3–6] (more discussions and references on this subject are given in the recent work [7]). With the limited ways of interpreting 0^+ excitations it is even more surprising to see the large and still growing number of low-energy 0^+ levels displaying widely differing properties. For example, the recent work [8] reports 20 excited 0^+ in just one nucleus, ^{112}Pd. This situation calls for new interpretations of excited levels 0^+ in even-even nuclei.

Particularly intriguing are 0^+ levels with very low excitation energies. The second 0^+ level in ^{98}Sr, identified by Schussler *et al.* [9] at 215.4 keV, is the lowest known excited 0^+ level in even-even nuclei. An analogous 0_2^+ level in ^{100}Zr is observed at 331.1 keV [10]. The proximity of 0_1^+ and 0_2^+ levels in ^{98}Sr and ^{100}Zr indicates their weak interaction and different structures. The latter is also indicated by the fact that ground states in both nuclei are deformed while 0_2^+ levels are spherical (see, e.g., Fig. 8 in Ref. [11]). Low excitation energies of 0_2^+ levels in ^{98}Sr and ^{100}Zr indicate that these levels do not correspond to any kind of surface vibrations.

Properties of 0_1^+ and 0_2^+ levels in ^{98}Sr and ^{100}Zr are different than in the nearby Ru isotopes, as shown in Fig. 1. The data points for Ru isotopes shown in panel (a) display a characteristic pattern of the so-called avoided crossing [12]. The two-level-mixing calculation [solid line in Fig. 1(a)], suggests strong interaction of $V \approx 400$ keV [13] between 0_1^+ and 0_2^+ levels in Ru isotopes. For Sr isotopes, shown in Fig. 1(b), the picture is different. In ^{98}Sr the interaction strength between the 0_1^+ and 0_2^+ levels is an order of magnitude lower [1,9] and the "crossing" in Sr isotopes takes place at higher neutron number, as compared to Ru isotopes.

The key questions are, what is the structure of 0_2^+ excitations and what is the microscopic mechanism responsible for the evolution of these levels in the mass $A \approx 100$ region? The pronounced difference between the Ru and Sr isotopes in Fig. 1, showing a sudden onset of deformation in Sr isotopes at $N = 60$, more abrupt than in Ru isotopes, suggests that there is more than one mechanism at work. In the present work we report new data on 0_2^+ bands in ^{98}Sr and ^{100}Zr and discuss them in a wider context of 0^+ excitations in the mass $A \approx 100$ region, proposing new interpretations for 0^+ levels as well as new mechanisms for shape changes in the region.

After the Introduction we present in Sec. II the measurements performed and the new experimental results obtained in this work for ^{98}Sr and ^{100}Zr. In Sec. III the new data are discussed together with other excited 0^+ levels in the region and

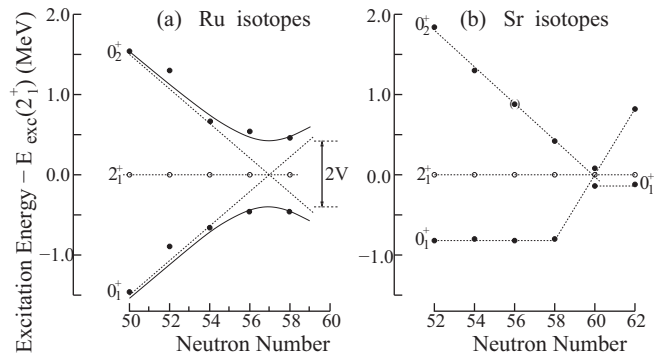

FIG. 1. Energies of 0_1^+ and 0_2^+ levels (full dots), relative to the 2_1^+ excitation (open dots) in (a) Ru and (b) Sr isotopes. Solid lines in (a) represent a two-level mixing calculation [13]. The experimental data are taken from Refs. [13,14]. Dotted lines are drawn to guide the eye. See text for further explanation.

 ©2019 American Physical Society

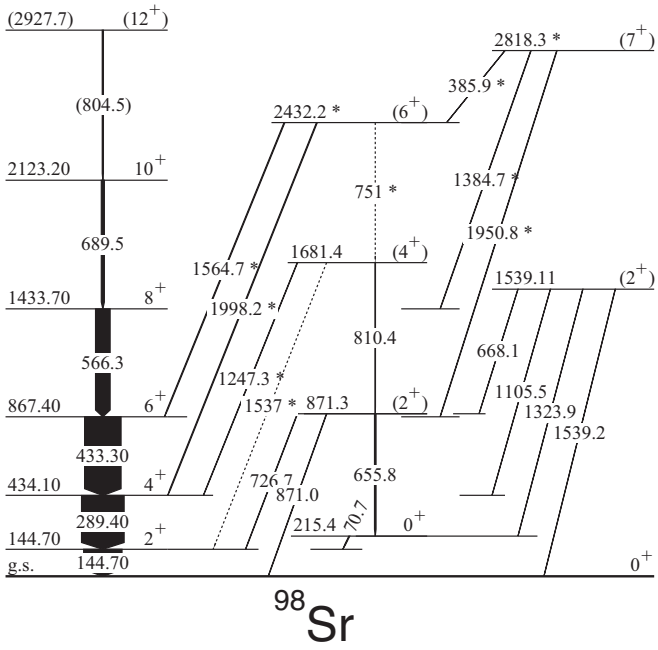

FIG. 2. Partial level scheme of ^{98}Sr obtained in this work in measurements of γ rays from spontaneous fission of ^{248}Cm and ^{252}Cf. New levels and transitions are marked with asterisks.

new interpretations are proposed. Section IV summarizes the work and outlines perspectives of further studies in the field.

II. MEASUREMENTS AND RESULTS

New experimental results on 0_2^+ bands in ^{98}Sr and ^{100}Zr were obtained from enhanced analysis of the data collected in measurements of γ rays following spontaneous fission of ^{248}Cm and ^{252}Cf, performed using the Eurogam2 [15] and Gammasphere [16] arrays, respectively. Both experiments were described in previous papers (see, e.g., Refs. [17–20]). These measurements were used before to study ^{98}Sr [21–23]. The ^{100}Zr nucleus was studied before using the data from another measurement of γ rays following spontaneous fission of ^{248}Cm, performed using the Eurogam I array [24], which was also used to study ^{98}Sr [25]. The present enhanced analysis, involving new sorting of multiple-γ coincidences into various three-dimensional histograms with higher resolution, as compared to the previous studies, as well as newly developed techniques of angular correlations [26], allowed the observation of new transitions and levels and unique determination of spins and parities for many levels in ^{98}Sr and ^{100}Zr.

A. Excitations in ^{98}Sr

The excitation scheme of ^{98}Sr was studied before in β-decay measurements [9,27–30] and measurements of γ rays following spontaneous fission of ^{248}Cm [22,25] and ^{252}Cf [31–33] and neutron-induced fission of ^{235}U [34].

Figure 2 shows partial level scheme of ^{98}Sr with a band on top of the 0_2^+, 215.4-keV level, as observed in this work. Table I lists energies and intensities of γ lines and energies of excited levels. Precise angular correlations from the Gammasphere measurement [26] obtained for γ-γ cascades of ^{98}Sr

TABLE I. Energies and intensities of γ lines in ^{98}Sr and ^{100}Zr from spontaneous fission of ^{248}Cm, as observed in this work.

E_γ (keV)	I_γ (rel.)	E_{exc} (keV)	E_γ (keV)	I_γ (rel.)	E_{exc} (keV)
	^{98}Sr			^{100}Zr	
70.7(3)	1.5(7)	215.4(3)	493.55(5)	1.3(2)	3019.6(1)
144.70(5)	100(4)	144.70(5)	497.36(5)	60(3)	1061.80(8)
289.40(5)	111(4)	434.10(9)	536.05(5)	3.2(3)	1414.9(1)
385.9(3)	0.6(3)	2818.3(2)	547.00(5)	2.8(3)	1961.9(1)
433.30(5)	95(5)	867.40(12)	547.5(1)	1.0(2)	878.85(7)
566.3(1)	38(5)	1433.70(15)	564.2(1)	0.9(2)	2526.1(1)
655.8(4)	1.0(5)	871.3(2)	615.8(1)	0.4(2)	3635.4(2)
689.5(2)	8(1)	2123.20(25)	617.65(8)	1.4(2)	2579.50(9)
726.7(3)	0.9(3)	871.3(2)	625.55(5)	27(3)	1687.35(9)
751.0(5)	0.5(3)	2432.2(2)	666.23(7)	2.9(3)	878.85(7)
804.5(3)	4(2)	2927.8(4)	709.5(3)	0.7(2)	3289.0(4)
810.4(4)	1.0(5)	1681.4(2	715.6(2)	0.5(2)	2130.6(2)
871.0(3)	2(1)	871.3(2)	739.0(1)	15(3)	2426.4(2)
1247.3(2)	0.7(3)	1681.4(2)	741.6(4)	0.2(1)	4377.0(5)
1384.7(2)	0.9(3)	2818.3(2)	841.7(2)	8(2)	3268.1(3)
1537.0(5)	0.5(3)	1681.4(2)	850.24(5)	5.1(5)	1414.9(1)
1564.7(2)	2.2(4)	2432.2(2)	862.8(3)	0.2(1)	3289.0(4)
1950.8(3)	1.1(3)	2818.3(2)	878.8(1)	1.4(2)	878.85(7)
1998.2(2)	1.2(3)	2432.2(2)	892.15(5)	1.0(3)	2579.50(9)
			900.00(5)	2.5(3)	1961.85(8)
	^{100}Zr		1202.2(2)	0.6(2)	1414.90(7)
118.65(5)	1.3(2)	331.32(7)	1209.1(3)	0.4(2)	3635.4(2)
212.67(3)	100(4)	212.67(4)	1332.15(7)	2.5(5)	3019.6(1)
351.99(3)	88(3)	564.66(5)	1464.25(7)	2.0(3)	2526.1(1)
395.6(1)	0.2(1)	2526.1(1)	1566.05(15)	0.7(2)	2130.6(2)
440.15(7)	0.4(1)	3019.6(1)			

are shown in Table II. These correlations uniquely determine spins in the ground-state cascade up to $I = 10$, confirming tentative assignments for the 867.40-, 1433.70-, and 2123.20-keV levels reported in the compilation [35]. Positive parity is adopted because of prompt, quadrupole character, thus an $E2$ multipolarity of transitions in this cascade. Table III shows $B(E2)$ rates in relative units calculated using branching ratios from Table I and mixing ratios from Table II.

We confirm known 871.3- and 1681.4-keV levels in ^{98}Sr [35] and add new decays of 1247.3 and 1537 keV from these levels. New transitions of 751, 1564.7, and 1998.2 keV define a new level at 2432.2 keV. We propose that this level also belongs to the 0_2^+ band, considering relative $B(E2)$ rates shown in Table III. The observed branchings, together with the predominant population of yrast and near-yrast levels in fission fragments [36], suggest spin-parity assignments of 2^+, 4^+, and 6^+ to the 871.3-, 1681.4-, and 2432.2-keV levels, respectively. This is also consistent with decay branchings of the new level at 2818.3 keV. To assist further discussion we have included in the scheme the 1539.11-keV level with its decays, as reported in the compilation [35].

B. Excitations in ^{100}Zr

The excitation scheme of the ^{100}Zr nucleus was studied before in β-decay measurements [10,37,38], which reported

TABLE II. Angular correlation coefficients for γ-γ cascades in ^{98}Sr and ^{100}Zr following fission of ^{252}Cf or ^{248}Cm$^{(a)}$. Label "sum" denotes summed correlations with all quadrupole transitions below $E_{\gamma 1}$.

$E_{\gamma 1}$-$E_{\gamma 2}$ cascade	A_2/A_0 exp.	A_4/A_0 exp.	Spins in cascade	$\delta^{\exp}(E_{\gamma 1})$
^{98}Sr				
289.40–144.70	0.092(9)	0.015(15)	4 - 2 - 0	
433.30–289.40	0.101(10)	0.019(15)	6 - 4 - 2	
566.3–433.30	0.121(17)	−0.019(27)	8 - 6 - 4	
689.5-sum	0.090(18)	0.024(26)	10 - 8 - 6	
^{100}Zr				
351.99–212.67	0.100(7)	0.010(9)	4 - 2 - 0	
497.36–351.99	0.107(7)	0.010(10)	6 - 4 - 2	
625.55–497.36	0.111(11)	0.019(16)	8 - 6 - 4	
739.0–497.36	0.107(17)	0.003(25)	10 - 8 - 6	
850.24-sum	−0.109(9)	0.080(14)	4 - 4 - 2	0.99(6)
			5 - 4 - 2	No solution
			6 - 4 - 4	No solution
900.00-sum	−0.017(15)	0.026(21)	6 - 6 - 4	0.74(7)
			7 - 6 - 4	0.09(3)
			8 - 6 - 4	No solution
1332.15-sum	−0.086(31)	−0.023(47)	8 - 8 - 6	No solution
			9 - 8 - 6	0.02(5)
			10 - 8 - 6	No solution
1464.25-sum	−0.057(19)	0.014(30)	6 - 6 - 4	0.92(12)
			7 - 6 - 4	0.02(3)
			8 - 6 - 4	No solution
1464.25-sum$^{(a)}$	−0.037(17)	0.040(30)	6 - 6 - 4	0.84(10)
			7 - 6 - 4	0.05(3)
			8 - 6 - 4	No solution
1566.05-sum	−0.076(59)	0.005(87)	4 - 4 - 2	1.0(4)
			5 - 4 - 2	−0.01(9) or 25(18)
			6 - 4 - 2	No solution

TABLE III. Relative $B(E2)$ values for $E2$ decays of levels in ^{98}Sr and ^{100}Zr, calculated using γ branchings and mixing ratios observed in this work.

$E_{\rm exc}$ (keV)	E_γ (keV)	$B(E2)$ (rel.)	$E_{\rm exc}$ (keV)	E_γ (keV)	$B(E2)$ (rel.)
	^{98}Sr			^{100}Zr	
871.3	655.8	100(50)	878.85	547.5	100(20)
	871.0	48(24)		878.8	13(2)
1681.4	810.4	100(50)	1414.90	536.05	100(10)
	1537	2.0(1.2)		850.24	8(1)
				1202.2	0.3(1)
2432.2	751	100(60)	1961.85	547.00	100(11)
	1998.2	1.8(5)		900.00	2.6(5)
			2526.1	395.6	100(50)
				1464.25	0.3(1)
			3019.6	493.55	100(16)
				1332.15	0.001(2)

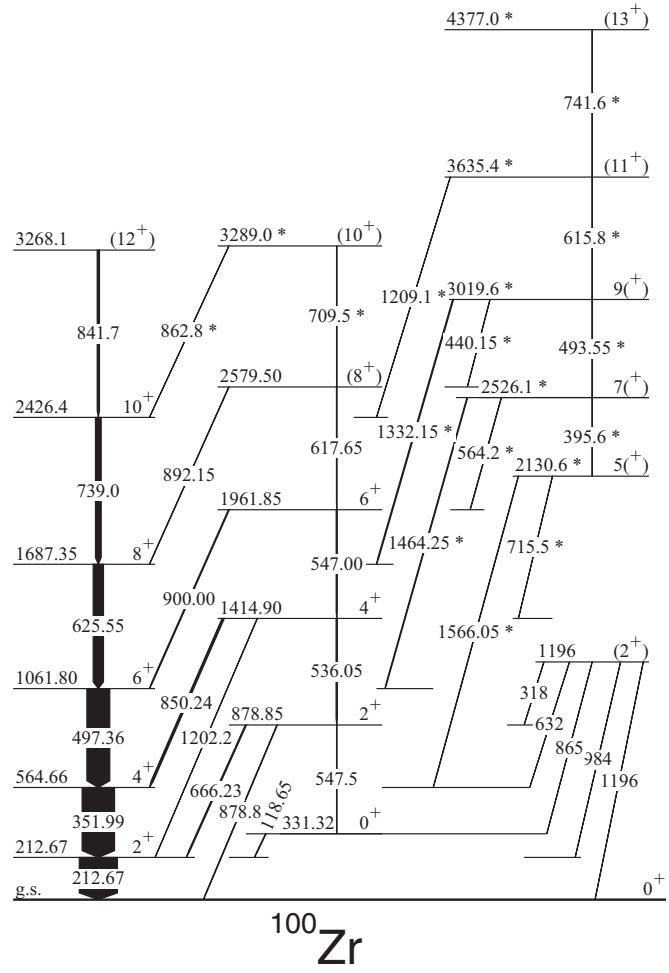

FIG. 3. Partial level scheme of ^{100}Zr obtained in this work in measurements of γ rays from spontaneous fission of ^{248}Cm and ^{252}Cf. New or reassigned levels and transitions, compared to Refs. [39–41], are marked with asterisks.

the 0_2^+ level, and in measurements of γ rays following spontaneous fission of ^{248}Cm [25] and ^{252}Cf [39] as well as α-induced fission of ^{238}U [40].

Figure 3 shows a partial excitation scheme of ^{100}Zr with a band on top of the 0_2^+, 331.32-keV level, as observed in this work. Table I shows energies and intensities of γ lines and energies of excited levels. In Table II angular correlation coefficients for γ-γ cascades in ^{100}Zr are shown. The correlations determine uniquely spins of the 564.66- 1061.80-, 1687.35-, and 2426.5-keV levels of the ground-state band, confirming tentative assignments reported in the compilation [41]. Positive parity is adopted because of prompt, quadrupole character, thus an $E2$ multipolarity of transitions in this cascade.

The 878.85-keV, 2_2^+ level was reported in Ref. [10]. The 0_2^+ band was extended to higher spins in Ref. [39]. In this work we have rearranged and extended this band, using angular correlations shown in Table II to determine spins and parities of the level in the band on top of the 0_2^+ level. We confirm up to spin (8^+) the 0_2^+ band, reported in Ref. [39] as band

(4), adding a new 1202.2-keV decay from the 1414.90-keV level. The 1397.1-keV decay from the 1961.85-keV level is not confirmed. We introduce a new (10^+) band member of the 0_2^+ band at 3289.0 keV instead of the 3019.6-keV level reported in [39].

Angular correlations involving the 850.24-keV transition determine uniquely spin $I = 4$ of the 1414.90-keV level. Positive parity for this level is inferred from the large mixing ratio, δ, of the prompt 850.24-keV transition. Consequently, the prompt 536.05–878.8-keV $\gamma\gamma$ cascade indicates spin-parity 2^+ for the 878.85-keV level. Similarly, the prompt 547.00–536.05-keV cascade indicates spin-parity 6^+ for the 1961.85-keV level, considering the possible solutions listed in Table II for the 900.00-keV transition.

The 3019.6-keV level has spin $I = 9$, as indicated by angular correlations for the prompt 1332.15- and 1464.25-keV transitions, shown in Table II, and by the "yrast-population" argument [36]. The 3019.6-keV level belongs to a new band to which we assign also the 2526.1- and 3635.4-keV levels reported in [39] and add new levels at 2130.6 and 4377.0 keV. New in-band decays of 395.6, 493.55 and 741.5 keV as well as new out-of-band decays of 1566.05 and 715.5 keV are introduced. The previously reported 440.15-, 564.2-, 1209.1-, 1332.15-, and 1464.25-keV γ transitions reported in [39] are now out-of-band decays of the new band. Angular correlations for the 1332.15-, 1464.25-, and 1566.05-keV transitions give consistent and unique spin assignments to the 2130.6-, 2526.1-, and 3019.6-keV levels, as shown in Fig. 3. The data in Table III support the new band identification.

To assist further discussion we have included in the scheme the known 1196-keV level with its decays [41].

III. DISCUSSION

Looking for an interpretation of 0_2^+ excitations in ^{98}Sr and ^{100}Zr, one observes that the present data show that bands on top of these levels are clearly not of rotational nature. In this respect they are very different from ground-state bands in both nuclei. On the other hand one observes numerous decays from *all* levels in 0_2^+ bands to levels in ground-state bands. This suggests some underlying similarity of the two structures which, however, does not result in strong band mixing, as shown in Fig. 1.

In Ref. [9] excitation energies and branchings were used to extract the interaction strength between the 0_1^+ and 0_2^+ bands in ^{98}Sr. This was analyzed further using transition rates as summarized in Ref. [42], which points to significant differences between various works. The present data suggest a reevaluation, indicating that the assumption of the "rotational" character of the 0_2^+ band or the selection of levels which mix [9,30,31,43–46] should be reconsidered. Furthermore, the (2^+) levels at 1539.11 and 1196 keV in ^{98}Sr and ^{100}Zr nuclei, respectively, which are most likely collective structures, are also linked to both 0_1^+ and 0_2^+ bands in the two nuclei, suggesting that the mixing scenario may by even more complex.

With these reservations in mind one may, nevertheless, conclude the quasivibrational character, hence low deformation, of 0_2^+ bands in ^{98}Sr and ^{100}Zr as well as their weak interaction with 0_1^+ bands, which is about an order of magnitude lower than in Ru isotopes, as summarized in Table VI of Ref. [1].

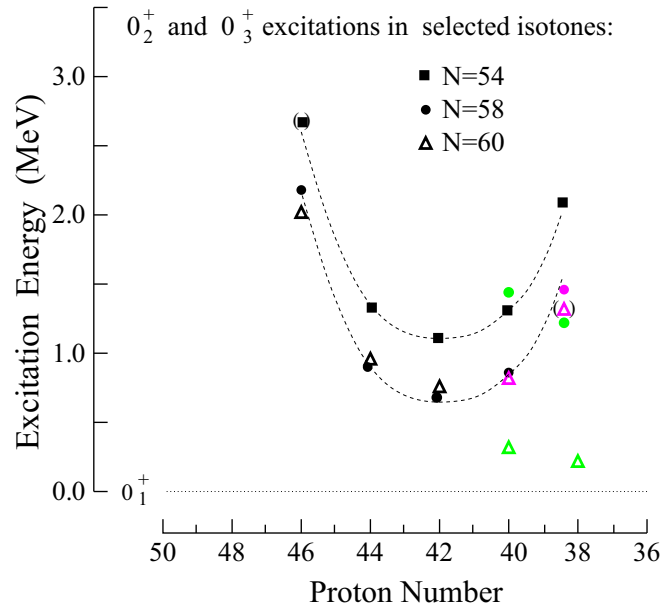

FIG. 4. Excitation energies of 0_2^+ levels relative to the 0_1^+ ground state in the $N = 54$, 58, and 60 isotones. In addition, energies of 0_3^+ levels in ^{96}Sr, ^{98}Sr, and ^{100}Zr (in magenta color) and in ^{98}Zr (green circle) are shown. See text for the description of dashed lines and the points shown in green. The experimental data are taken from Ref. [14]. Points in parentheses have tentative spin assignments.

A. Systematics of 0^+ excitation energies

To find more information about the nature of 0_2^+ levels in ^{98}Sr and ^{100}Zr we show in Fig. 4 excitation energies for 0_2^+ levels, starting with selected isotones, to keep the picture simple. At $N = 54$ (filled squares) one observes a regular "parabolic" dependence on the proton number (dashed line drawn to guide the eye). The same curve shifted down by 450 keV fits points at $N = 58$ (filled circles) and $N = 60$ (triangles), suggesting that this type of dependence may be universal in the region. However, there is a distinct exception. The 0_2^+ levels in ^{98}Sr and ^{100}Zr (green triangles) fall well below the lower "parabola," which fits better 0_3^+ levels (magenta triangles) in both nuclei. Also the 0_3^+ level in ^{96}Sr (magenta circle) fits the $N = 58$ trend better than the 0_2^+ level (green circle) in this nucleus, though this is less evident. To keep the picture simple in Fig. 4 we do not show data for $N = 56$, which show extra exceptions, as will be discussed below.

The properties of 0^+ excitations from Fig. 4 are analyzed further in Fig. 5, this time against the neutron number, revealing further distinct features of the green points. In Fig. 5 we show, in addition, 0_2^+ levels from Fig. 1, including $N = 66$ as well as 0_2^+ levels in Zr and Mo isotopes and 0_3^+ levels in ^{94}Sr and ^{96}Zr ($N = 56$).

Figure 5 indicates that collectivity is growing with the increasing number of neutrons, which is reflected by the

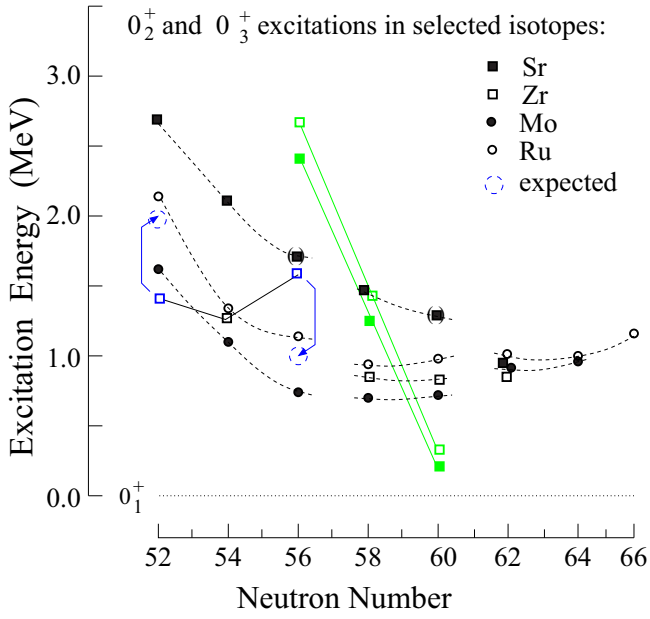

FIG. 5. Excitation energies of 0_2^+ and selected 0_3^+ levels relative to 0_1^+ states in Ru, Mo, Zr, and Sr isotopes. Data points in green at $N = 58$ and $N = 60$ are the same as in Fig. 4. See text for further comments on data points and lines drawn in the figure. The experimental data are taken from Ref. [14]. Points in parentheses have tentative spin assignments.

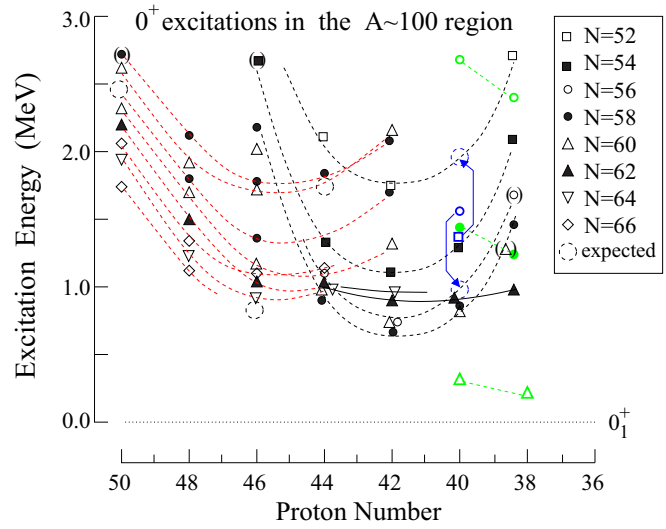

FIG. 6. Excitation energies of all 0_2^+ and most of 0_3^+ known levels and selected 0_4^+ levels in $A \approx 100$ nuclei, drawn relative to the respective 0_1^+, ground-state levels. The data are taken from Ref. [14]. A detailed explanation of symbols, lines, and colors is given in the text.

lowering of 0^+ excitation energies. In the figure the systematics for Ru isotopes (open circles) shows some discontinuity and we arrange them into three groups: with $N < 58$ where the neutrons fill predominantly the $d_{5/2}$ orbital, with $N = 58$ and 60 corresponding to filling the $g_{7/2}$ orbital, and with $N \geqslant 62$ where the $h_{11/2}$ orbital is filling [13]. The data points for Mo, Zr, and Sr are also grouped in this way. Out of 33 excited 0^+ levels in Fig. 5, 25 follow this trend. Two deviations (marked by blue arrows) at ^{92}Zr and ^{96}Zr (blue squares) from the trend are discussed further in the text. The remaining six points, shown in green color belong to another group, incorporating 0_2^+ levels in ^{96}Sr, ^{98}Sr, and ^{100}Zr and 0_3^+ levels in ^{94}Sr, ^{96}Zr, and ^{98}Zr. These points show a distinctly different dependence of their excitation energies on the neutron number, suggesting their different structure.

To learn more about the green points, we show in Fig. 6 the extended version of Fig. 4, displaying all 0_2^+ and most of 0_3^+ known levels from the $38 \leqslant Z \leqslant 50$, $52 \leqslant N \leqslant 66$ region. The 0_4^+ levels in ^{102}Mo and ^{106}Pd are also added to illustrate some extra features.

The "parabolic" trend seen in Fig. 4 is now even more evident. Black dashed lines copied from Fig. 4 systematize the data for $52 \leqslant N \leqslant 60$ isotones in the $38 \leqslant Z \leqslant 46$ range. We note that for ^{106}Pd it is the 0_4^+ level which fits best the $N = 60$ trend in this range, while the 0_2^+ and 0_3^+ levels of ^{106}Pd fit best the parabola-like curves drawn in red. The 0_3^+ and 0_4^+ levels in ^{102}Mo also fit better the red curves. The red curves systematize data points for $58 \leqslant N \leqslant 66$ isotones in the $42 \leqslant Z \leqslant 50$ range. Out of 63 data points in Fig. 6 only eight deviate from "parabolic" trends. Two 0_2^+ levels in ^{92}Zr and ^{96}Zr (drawn in blue color), which do not follow black curves (their expected positions on "parabolas" are marked by blue, dashed circles), show the same deviations as in Fig. 5. The increase in ^{96}Zr may be due to the $Z = 40$ or $N = 56$ subshell closures while the lowering in ^{92}Zr suggests that some extra effects contribute, like the proton-neutron mixing expected in this nucleus [47]. Six points shown in green color are the same as green points in Fig. 5. In Fig. 6 they are not assigned to any respective "parabolas," further suggesting their different character. We note that in the past the shape change in ^{98}Zr was associated with the 0_3^+ level [48,49], but deformed structures on top of this level were not confirmed [50]. A recent paper [51] reports a moderately deformed band in ^{98}Zr, incorporating the 1590-, 1843-, and 2491-keV levels. In our opinion, this confirms a deformed band based on the 0_2^+ level, proposed in Figs. 4 and 10 of Ref. [52]. The above suggests that the 0_3^+ level in ^{98}Zr is weakly deformed, similar to 0_2^+ levels in ^{98}Sr and ^{100}Zr.

The 0^+ excitations shown in Fig. 6 can be arranged into four groups:

(i) points following black dashed lines,
(ii) points following red dashed lines,
(iii) points shown in green color,
(iv) points following black solid lines.

This phenomenological classification, though rather arbitrary, is quite suggestive and deserves further comments.

B. New interpretation of shape evolution in the $A \approx 100$ region

The "parabolic" trend, analogous to the one describing groups (i) and (ii), was discussed in Ref. [53] and observed for 0_2^+ levels in Hg isotopes (Fig. 3.19 in [54] and Fig. 10 in Ref. [1]), where it was interpreted as due to a 2p-2h,

"intruder," i.e., promotion of a proton pair producing a low-energy, 0^+ excitation due to an attractive interaction of this pair with neutrons in a nearby neutron orbital [1]. The attraction, which varies with the changing neutron number, results in a "parabolic" trend of the 0_2^+ energy. By analogy, the "parabolic" trend in Fig. 6 can be understood as being due to the 2p-2h intruder state created by an excitation of a pair of neutrons from the $d_{5/2}$ orbital to the $g_{7/2}$ or $h_{11/2}$ orbital. This pair can then attract the $g_{9/2}$ proton particles (black "parabola") or the $g_{9/2}$ proton holes (red "parabola"). These two groups comprise most of the 0^+ levels in Fig. 6, suggesting that the 2p-2h intruder excitation is the dominant mechanism producing collectivity in the region.

The proton-neutron attraction increasing with the growing population of $g_{7/2}$ and $h_{11/2}$ neutron orbitals, explains the trend shown in Fig. 5 (except the green points). In this context the spin-orbit-partner effect of Federman and Pittel is supported; however, not for the ground-state 0^+ levels, as originally proposed [55–58], but for *excited* 0^+ levels. Such a conclusion has also been drawn from calculations of 0^+ levels in ^{96}Sr and ^{98}Zr [59]. In other words, there is no *type-II* phase transition in Sr and Zr isotopes, as already argued in Refs. [48,49,52,60].

At $N = 58$ weakly deformed bands based on the 0_2^+ level have been proposed in ^{96}Sr and ^{98}Zr (see Fig. 10 in Ref. [52]). The deformation is growing in such bands when the neutron number increases and is larger in ^{97}Sr and ^{99}Zr (see Fig. 9 of Ref. [52]), fitting the scheme of a *type-I* phase transition, as illustrated in Fig. 8 of Ref. [49]. This scenario was supported by calculations [61–63], where it was attributed to the population of the deformation-driving, $h_{11/2}$ neutron intruder, with further refinements discussed in Refs. [11,52,64,65]. However, the present work suggests that the deformation-change process in Sr and Zr isotopes may be even more complex.

We suggest that the increased collectivity in 0^+ excited levels of Sr and Zr, located on the "parabolas" in Fig. 6, which is due to proton-neutron attraction, is passed to ground-state 0_1^+ levels, similar to what is observed in Ru isotopes [13]. Thus, instead of a type-I phase transition one observes rather the avoided crossing in most of the nuclei of the $A \approx 100$ region. However, as seen in Ru isotopes, such a crossing induces a less abrupt shape change than the one observed in Sr and Zr isotopes. This is illustrated in Fig. 7(a), where the change of β_2 deformation parameter of 0_1^+ levels in Sr and Zr isotopes (continuous cyan line) is compared to an analogous change in Ru isotopes (continuous red line). Therefore an extra effect, enhancing and accelerating the shape-change process, is needed for Sr and Zr isotopes. The picture is further complicated by the appearance of the very low-lying 0_2^+ levels in ^{98}Sr and ^{100}Zr [group (iii)].

Analogies with 0^+ excitations in the $A \approx 150$ region, where a sudden change of deformation occurs, may provide further hints about the shape-change mechanism in the $A \approx 100$ region as well as the nature of levels from group (iii). The weakly deformed 0_3^+ level in ^{154}Gd was interpreted by Kulp *et al.* [66] as the so-called pairing isomer' involving the $11/2^-[505]$ Nilsson "extruder." Interestingly, the 0_2^+ deformed configuration in ^{154}Gd was also associated with the $11/2^-[505]$ Nilsson orbital, and was interpreted by

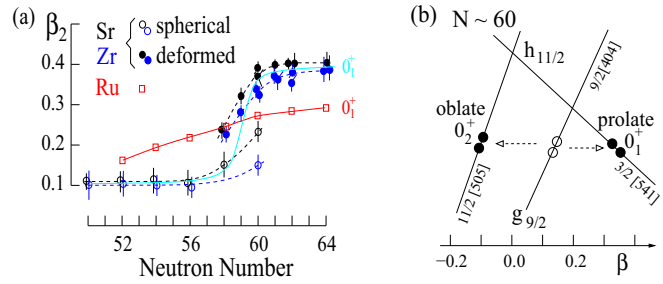

FIG. 7. (a) Evolution of the β_2 deformation parameter for 0_1^+ and 0_2^+ levels in Sr, Zr, and Ru isotopes. Thick, continuous lines follow 0_1^+ configurations in Sr and Zr (cyan) and Ru (red) isotopes. Dashed lines follow spherical or deformed configurations in Sr (black) or Zr (blue) isotopes. The data are from Refs. [11,14,52]. (b) Schematic explanation of the extruder 2p-2h excitations around $N = 60$, involving the $\nu 9/2^+[404]$ extruder.

Sharpey-Schafer *et al.* [5] as a configuration with the leading component due to an excitation of a pair of neutrons from the upsloping $11/2^-[505]$ extruder orbital to the downsloping $3/2^+[651]$ intruder orbital. Such a 2p-2h configuration corresponds to the so called pairing isomer, involving two $11/2^-[505]$ holes, as proposed by Garrett *et al.* [4]. The presences of the $11/2^-[505]$ extruder, associated with deformed bands in odd-A nuclei of the region, is well documented (see, e.g., Fig. 5 in Ref. [67] or Fig. 6 in Ref. [68]). While these interpretations may need further attention, considering that the 0_1^+ ground state, which is the most deformed configuration in ^{154}Gd, also needs an explanation, there is convincing evidence of the $11/2^-[505]$ neutron extruder being involved in generating various configurations in the $A \approx 105$ region. This applies also to the 0_2^+ deformed configurations, as indicated by the correlation between excitation energies of these states and $11/2^-$ levels in odd-A neighboring nuclei, shown in Fig. 11 of Ref. [6].

Effects, analogous to those discussed above for the $A \approx 150$ nuclei may be expected in the $A \approx 100$ region, and in this work we employ the "extruder mechanism" to explain the sudden increase of deformation in 0_1^+ levels of even-even nuclei at $N = 60$. Figure 7(b) schematically illustrates how a deformed configuration could be produced in even-even nuclei of the the $A \approx 100$ region by shifting a pair of neutrons from the upsloping $9/2^+[404]$ extruder to the downsloping $3/2^-[541]$ intruder orbital, both orbitals being present at the Fermi level around $N = 60$ (see, for example, the Nilsson diagram in Fig. 9 of Ref. [69]). Because in ^{98}Sr and ^{100}Zr no excited 0^+ deformed levels are observed, we propose that in both nuclei this 2p-2h neutron configuration is the leading contribution of the 0_1^+ deformed ground state. The presence of the $9/2^+[404]$ extruder orbital around $N = 60$ in the $A \approx 100$ region is well documented in deformed bands of odd-A nuclei [11,19,64,69–72] and in two-quasiparticle, deformed bands of even-even nuclei [29,39,40,52,73].

To interpret weakly deformed 0_2^+ levels of group (iii), we note that for four decades theoretical works have been predicting the existence of oblate 0^+ excitations in these nuclei [59,74,75]. The Nilsson diagram for this region (see,

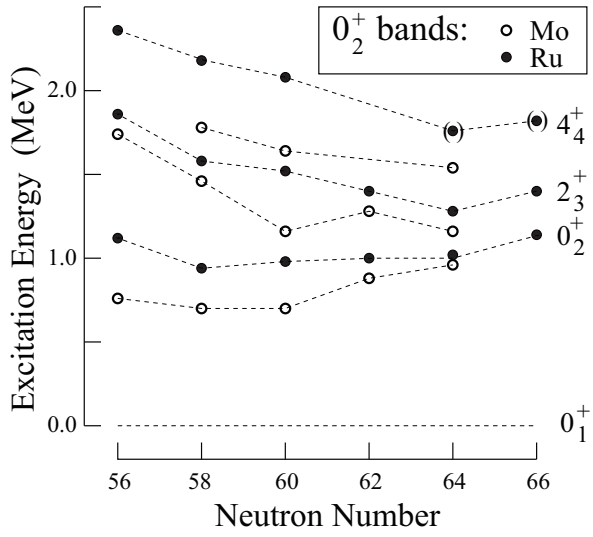

FIG. 8. Bands on top of 0_2^+ levels in Mo and Ru isotopes. Lines are drawn to guide the eye. The data points are from Refs. [13,14,77].

e.g., Fig. 9 in Ref. [69]) shows a concentration of orbitals on the oblate side at an energy close to the Fermi level, where the orbits are active on the prolate side. The $11/2^-[505]$ downsloping orbital is the distinct member of this oblate bunch, and its population could account for the discussed 0_2^+ levels in ^{98}Sr and ^{100}Zr, as schematically shown in Fig. 7(b). The picture explains the deformation difference between 0_1^+ and 0_2^+ configurations in ^{98}Sr and ^{100}Zr discussed above. In support of the oblate shape, the recent work [76] reports a weakly deformed $11/2^-$ oblate configuration in ^{99}Zr, based on the $h_{11/2}$ neutron orbital, coexisting with the prolate structures in this nucleus, where the $9/2^+[404]$ extruder has been observed for the first time in the $A \approx 100$ region. It is then possible that in the even-even neighbors the two neutrons are passed from the $9/2^+[404]$ extruder to the $11/2^-[505]$ oblate intruder. If so, the leading 2p-2h term in both 0_1^+ and 0_2^+ configurations would have a common $(\nu 9/2^+[404])^{-2}$ component, explaining multiple decays of 0_2^+ bands to 0_1^+ bands, seen in Figs. 2 and 3. Furthermore, the sudden increase of the deformation in 0_1^+ levels and the appearance of low 0_2^+ levels at $N = 60$ would correlate with the local approach of the $\nu 9/2^+[404]$ extruder to the Fermi surface at this neutron number.

Finally, we will discuss 0^+ excitations of group (vi). In Fig. 8 one can see that above neutron number $N = 60$ the cascade on top of the 0_2^+ level in Ru and Mo isotopes evolves into a rotational band. At $N > 60$ one expects the dominant role of $h_{11/2}$ neutrons in creating deformation in ground state levels of Mo and Ru isotopes. As discussed in Ref. [13], at $N < 60$ 0_1^+ and 0_2^+ levels mix and the deformation is passed from the 0_2^+ level to the 0_1^+ ground state. It is likely that above $N = 60$ the 0_1^+ and 0_2^+ also mix but now the deformation of the 0_1^+ ground state, which is more deformed, is passed to 0_2^+ level. Such mixing would imply structural similarity of 0_1^+ and 0_2^+ levels, consistent with the rather flat dependence of the 0_2^+ excitation energy on the proton number (solid black line in Fig. 6). Thus, instead of being 2p-2h neutron structures interacting with $g_{9/2}$ protons and showing a characteristic parabolic dependence on the proton number, 0_2^+ levels at $N > 60$ are probably vibrations on top of the 0_1^+ ground states. Furthermore, as seen in Fig. 8, at $N > 60$ excitation energy of 0_2^+ levels grows to more than 1 MeV and it is possible that these levels become heads of so-called β bands. In ^{110}Ru$_{66}$ this is further hinted by the predominant decay of the 0_2^+ level to the 2_1^+ level of the ground state [78].

IV. SUMMARY AND PERSPECTIVES

In summary, excited levels in ^{98}Sr and ^{100}Zr were studied using data from measurements of γ rays following spontaneous fission of ^{248}Cm and ^{252}Cf, performed with the Eurogam2 and Gammasphere multidetector arrays, respectively. Vibrational bands on top of 0_2^+ levels in ^{98}Sr and ^{100}Zr, reevaluated and extended in this work, are interpreted as oblate structures with intruder-type 2p-2h dominant configuration, containing two neutrons in the $11/2^-[505]$ oblate intruder and two neutron holes in the $9/2^+[404]$ prolate extruder orbital, respectively. Highly deformed, 0_1^+ ground states in both nuclei are interpreted as a prolate structure with intruder-type 2p-2h dominant configuration containing two neutrons in a low-Ω orbital originating from the $\nu h_{11/2}$ shell and two neutron holes in the $9/2^+[404]$ prolate extruder orbital. The latter, prolate-deformed configuration, which appears around $N = 60$, is superimposed on the gradual increase of the deformation observed in most nuclei of the $A \approx 100$ region. This gradual increase is due to another intruder-type 2p-2h neutron configuration, where two neutrons are excited from the $d_{5/2}$ shell to the $g_{7/2}$ or $h_{11/2}$ shell. When promoted, these two neutrons interact attractively with protons in the $g_{9/2}$ shell. The local approach of the $9/2^+[404]$ extruder to the Fermi level at $N \approx 60$ explains the local character of both the sudden increase of deformation and the local appearance of low-energy 0_2^+ levels in the ^{98}Sr and ^{100}Zr nuclei. We also propose that above $N = 60$ the 0_2^+ excitations, which show there slowly increasing excitation energies, may evolve into β vibrational states, explaining, for example, the regular $K^\pi = 0^+$ rotational band based on the 1137-keV level in ^{110}Ru.

The phenomenological classification of 0^+ excitations in the $A \approx 100$ region, offering new interpretation of these excitations, needs further verification. In Fig. 6 we have marked with black dashed circles three unknown but expected 0^+ excitations (0_2^+ levels in ^{108}Sn and ^{112}Pd and 0_3^+ level in ^{104}Ru). Finding these excitations at suggested energies would be an important confirmation of the proposed systematics. Other observables should be studied as well, to check if points on a given parabola have deeper structural relations. One needs here, first of all, measurements of particle transfer cross sections and electromagnetic moments of levels and transitions.

ACKNOWLEDGMENTS

This work is supported by the Polish National Science Centre under the contract DEC-2013/09/B/ST2/03485. The authors are indebted for the use of ^{248}Cm to the Office of

Basic Energy Sciences, U.S. Department of Energy, through the transplutonium element production facilities at the Oak Ridge National Laboratory. The authors acknowledge fruitful discussions with Janusz Skalski and John Wood.

[1] K. Heyde and J. L. Wood, Rev. Mod. Phys. **83**, 1467 (2011).
[2] A. Bohr and B. R. Mottelson, *Nuclear Structure, Volume II: Nuclear Deformations* (Benjamin, New York, 1975).
[3] P. E. Garrett, J. Phys. G: Nucl. Part. Phys. **27**, R1 (2001).
[4] P. E. Garrett, W. D. Kulp, J. L. Wood, D. Bandyopadhyay, S. Choudry, D. Dashdorj, S. R. Lesher, M. T. McEllistrem, M. Mynk, J. N. Orc, and S. W. Yates, Phys. Rev. Lett. **103**, 062501 (2009).
[5] J. F. Sharpey-Schafer, S. M. Mulins, R. A. Bark, J. Kau, F. Komati, E. A. Lawrie, J. J. Lawrie, T. E. Madiba, P. Maine, A. Minkova, S. H. T. Murray, N. J. Ncapayi, and P. A. Vymers, Eur. Phys. J. A **47**, 5 (2011).
[6] J. F. Sharpey-Schafer, R. A. Bark, S. P. Bvumbi, T. R. S. Dinoko, and S. N. T. Majola, Eur. Phys. J. A **55**, 15 (2019).
[7] A. Leviatan, N. Gavrielov, J. E. Garcia-Ramos, and P. Van Isacker, Phys. Rev. C **98**, 031302(R) (2018).
[8] D. S. Jamieson, P. E. Garrett, G. C. Ball, G. A. Demand, T. Faestermann, P. Finlay, K. L. Green, R. Hertenberger, K. G. Leach, A. A. Phillips, C. S. Sumithrarachchi, S. Triambak, and H.-F. Wirth, Phys. Rev. C **98**, 044309 (2018).
[9] F. Schussler, J. A. Pinston, E. Monnand, A. Moussa, G. Jung, E. Koglin, B. Pfeiffer, R. V. F. Janssens, and J. van Klinken, Nucl. Phys. A **339**, 415 (1980).
[10] T. A. Khan, W. D. Lauppe, K. Systemich, H. Lawin, G. Sadler, and H. A. Selic, Z. Phys. A **283**, 105 (1977).
[11] W. Urban, J. A. Pinston, J. Genevey, T. Rząca-Urban, A. Złomaniec, G. Simpson, J. L. Durell, W. R. Phillips, A. G. Smith, B. J. Varley, I. Ahmad, and N. Schulz, Eur. Phys. J. A **22**, 241 (2004).
[12] L. D. Landau and E. M. Lifshitz, *Quantum Mechanics: Non-Relativistic Theory*, 3rd ed. (Elsevier, New York, 1981).
[13] W. Urban, M. Jentschel, R. F. Casten, J. Jolie, Ch. Bernards, B. Maerkisch, Th. Materna, P. Mutti, L. Próchniak, T. Rząca-Urban, G. S. Simpson, V. Werner, and S. Ahmed, Phys. Rev. C **87**, 031304(R) (2013).
[14] ENSDF, 2018, www.nndc.bnl.gov.
[15] P. J. Nolan,, F. A. Beck, and D. B. Fossan, Ann. Rev. Nucl. Part. Sci. **44**, 561 (1994).
[16] I.-Y. Lee, Nucl. Phys. A **520**, c641 (1990).
[17] W. Urban, M. A. Jones, C. J. Pearson, I. Ahmad, M. Bentaleb, J. L. Durell, M. J. Leddy, E. Lubkiewicz, L. R. Morss, W. R. Phillips, N. Schulz, A. G. Smith, and B. J. Varley, Nucl. Instrum. Methods A **365**, 596 (1995).
[18] T. Rząca-Urban, W. R. Phillips, J. L. Durell, W. Urban, B. J. Varley, C. J. Pearson, J. A. Shannon, I. Ahmad, C. J. Lister, L. R. Morss, K. L. Nash, C. W. Williams, M. Bentaleb, E. Lubkiewicz, and N. Schulz, Phys. Lett. B **348**, 336 (1995).
[19] W. Urban, M. Czerwiński, J. Kurpeta, T. Rząca-Urban, J. Wiśniewski, T. Materna, L. W. Iskra, A. G. Smith, I. Ahmad, A. Blanc, H. Faust, U. Köster, M. Jentschel, P. Mutti, T. Soldner, G. S. Simpson, J. A. Pinston, G. de France, C. A. Ur, V.-V. Elomaa, T. Eronen, J. Hakala, A. Jokinen, A. Kankainen, I. D. Moore, J. Rissanen, A. Saastamoinen, J. Szerypo, C. Weber, and J. Aysto, Phys. Rev. C **96**, 044333 (2017).
[20] D. Patel, A. G. Smith, G. S. Simpson, R. M. Wall, J. F. Smith, O. J. Onakanmi, I. Ahmad, J. P. Greene, M. P. Carpenter, T. Lauritsen, C. J. Lister, R. F. Janssens, F. G. Kondev, D. Seweryniak, B. J. P. Gall, O. Dorveaux, and B. Roux, J. Phys. G. Nucl. Part. Phys. **28**, 649 (2002).
[21] A. G. Smith, J. L. Durell, W. R. Phillips, M. A. Jones, M. Leddy, W. Urban, B. J. Varley, I. Ahmad, L. R. Morss, M. Bentaleb, A. Guessous, E. Lubkiewicz, N. Schulz, and R. Wyss, Phys. Rev. Lett **77**, 1711 (1996).
[22] J. L. Durell, T. J. Armstrong, and W. Urban, Eur. Phys. J. A **20**, 97 (2004).
[23] A. G. Smith, J. L. Durell, W. R. Phillips, W. Urban, P. Sarriguren, and I. Ahmad, Phys. Rev. C **86**, 014321 (2012).
[24] J. L. Durell, W. R. Phillips, C. J. Pearson, J. A. Shannon, W. Urban, B. J. Varley, N. Rowley, K. Jain, I. Ahmad, C. J. Lister, L. R. Morss, K. L. Nash, C. W. Williams, N. Schulz, E. Lubkiewicz, and M. Bentaleb, Phys. Rev. C **52**, 2306(R) (1995).
[25] M. A. C. Hotchkis, J. L. Durell, J. B. Fitzgerald, A. S. Mowbray, W. R. Phillips, I. Ahmad, M. P. Carpenter, R. V. F. Janssens, T. L. Khoo, E. F. Moore, L. R. Morss, Ph. Benet, and D. Ye, Nucl. Phys. A **530**, 111 (1991).
[26] H. Naidja, F. Nowacki, B. Bounthong, M. Czerwiński, T. Rząca-Urban, T. Rogiński, W. Urban, J. Wiśniewski, K. Sieja, A. G. Smith, J. F. Smith, G. S. Simpson, I. Ahmad, and J. P. Greene, Phys. Rev. C **95**, 064303 (2017).
[27] H. Wollnik, F. K. Wohn, K. D. Wünsch, and G. Jung, Nucl. Phys. A **291**, 355 (1977).
[28] K. Becker, G. Jung, K.-H. Kobras, H. Wollnik, and B. Pfeiffer, Z. Phys. A **319**, 193 (1984).
[29] G. Lhersonneau, B. Pfeiffer, R. Capote, J. M. Quesada, H. Gabelmann, and K.-L. Kratz (ISOLDE Collaboration), Phys. Rev. C **65**, 024318 (2002).
[30] J. Park, A. B. Garnsworthy, R. Krücken, C. Andreoiu, G. C. Ball, P. C. Bender, A. Chester, A. Close, P. Finlay, P. E. Garrett, J. Glister, G. Hackman, B. Hadinia, K. G. Leach, E. T. Rand, S. Sjue, K. Starosta, C. E. Svensson, and E. Tardiff, Phys. Rev. C **93**, 014315 (2016).
[31] J. H. Hamilton, A. V. Ramayya, J. K. Hwang, J. Kormicki, B. R. S. Babu, A. Sandulescu, A. Florescu, W. Greiner, G. M. Ter-Akopian, Yu. Ts. Oganessian, A. V. Daniel, S. J. Zhu, M. G. Wang, T. Ginter, J. K. Deng, W. C. Ma, G. S. Popeko, Q. H. Lu, and H. C. Griffin, Prog. Part. Nucl. Phys. **38**, 273 (1997).
[32] M. L. Li, S. J. Zhu, J. H. Hamilton, A. V. Ramayya, J. K. Hwang, X. L. Che, Z. Zhang, Y. N. Y, R. C. Zheng, I. Y. Lee, J. O. Rasmussen, Y. X. Luo, and W. C. Ma, Chin. Phys. Lett. **21**, 2147 (2004).
[33] D. Fong, J. K. Hwang, A. V. Ramayya, J. H. Hamilton, C. J. Beyer, K. Li, P. M. Gore, E. F. Jones, Y. X. Luo, J. O. Rasmussen, S. J. Zhu, S. C. Wu, I. Y. Lee, P. Fallon, M. A. Stoyer, S. J. Asztalos, T. N. Ginter, J. D. Cole, G. M. Ter-Akopian, A. Daniel, and R. Donangelo, Eur. Phys. J. A **25**, 465 (2005).
[34] J.-M. Régis, J. Jolie, N. Saed-Samii, N. Warr, M. Pfeiffer, A. Blanc, M. Jentschel, U. Köster, P. Mutti, T. Soldner, G. S. Simpson, F. Drouet, A. Vancraeyenest, G. de France, E. Clément, O. Stezowski, C. A. Ur, W. Urban *et al.*, Phys. Rev. C **95**, 054319 (2017).

[35] B. Singh and Z. Hu, Nucl. Data Sheets **98**, 335 (2003).
[36] I. Ahmad and W. R. Phillips, Rep. Prog. Phys. **58**, 1415 (1995)
[37] T. A. Khan, W.-D. Lauppe, K. Systemich, H. Lawin, and H. A. Selic, Z. Phys. A **284**, 313 (1978).
[38] H. A. Selic, W. Borgs, W.-D. Lauppe, H. Lawin, and K. Systemich, Z. Phys. A **286**, 123 (1978).
[39] J. K. Hwang, A. V. Ramayya, J. H. Hamilton, J. O. Rasmussen, Y. X. Luo, D. Fong, K. Li, C. Goodin, S. J. Zhu, S. C. Wu, M. A. Stoyer, R. Donangelo, X.-R. Zhu, and H. Sagawa, Phys. Rev. C **74**, 017303 (2006).
[40] H. Hua, C. Y. Wu, D. Cline, A. B. Hayes, R. Teng, R. M. Clark, P. Fallon, A. Goergen, A. O. Macchiavelli, and K. Vetter, Phys. Rev. C **69**, 014317 (2004).
[41] B. Singh, Nucl. Data Sheets **109**, 297 (2008).
[42] H. T. Fortune, Nucl. Phys A **957**, 184 (2017).
[43] F. K. Wohn, J. C. Hill, C. B. Howard, K. Sistemich, R. F. Petry, R. L. Gill, H. Mach, and A. Piotrowski, Phys. Rev. C **33**, 677 (1986).
[44] H. Mach, M. Moszyński, R. L. Gill, F. K. Wohn, J. A. Winger, J. C. Hill, G. Molnar, and K. Sistemich, Phys. Lett. B **230**, 21 (1989).
[45] C. Y. Wu, H. Hua, and D. Cline, Phys. Rev. C **68**, 034322 (2003).
[46] E. Clément, M. Zielińska, A. Görgen, W. Korten, S. Péru, J. Libert, H. Goutte, S. Hilaire, B. Bastin, C. Bauer, A. Blazhev, N. Bree, B. Bruyneel *et al.*, Phys. Rev. Lett. **116**, 022701 (2016).
[47] V. Werner, D. Belic, P. von Brentano, C. Fransen, A. Gade, H. von Garrel, J. Jolie, U. Kneissl, C. Kohstall, A. Linnemann, A. F. Lisetskiy, N. Pietrala, H. H. Pitz, M. Scheck, K.-H. Speidel, F. Stedile, and S. W. Yates, Phys. Lett. B **550**, 140 (2002).
[48] R. K. Sheline, I. Ragnarsson, and.G. Nilsson, Phys. Lett. B **41**, 115 (1972).
[49] G. Lhersonneau, B. Pfeiffer, K.-L. Kratz, T. Enqvist, P. P. Jauho, A. Jokinen, J. Kantele, M. Leino, J. M. Parmonen, H. Penttilä, and J. Äystö (ISOLDE Collaboration), Phys. Rev. C **49**, 1379 (1994).
[50] J. H. Hamilton, A. V. Ramayya, S. J. Zhu, G. M. Ter-Akopian, Yu. Ts. Oganessian, J. D. Cole, J. O. Rasmussen, and M. A. Stoyer, Prog. Nucl. Part. Phys. **35**, 635 (1995).
[51] P. Singh, W. Korten, T. W. Hagen, A. Görgen, L. Grente, M.-D. Salsac, F. Farget, E. Clément, G. de France, T. Braunroth, B. Bruyneel, I. Celikovic, O. Delaune, A. Dewald, A. Dijon, J.-P. Delaroche, M. Girod, M. Hackstein, B. Jacquot, J. Libert, J. Litzinger, J. Ljungvall, C. Louchart, A. Gottardo, C. Michelagnoli *et al.*, Phys. Rev. Lett. **121**, 192501 (2018).
[52] W. Urban, J. L. Durell, A. G. Smith, W. R. Phillips, M. A. Jones, B. J. Varley, T. Rzça-Urban, I. Ahmad, L. R. Morss, M. Bentaleb, and N. Schulz, Nucl. Phys A **689**, 605 (2001).
[53] K. Heyde, P. Van Isacker, R. F. Casten, and J. L. Wood, Phys. Lett. B **155**, 303 (1985).
[54] J. L. Wood, K. Heyde, W. Nazarewicz, M. Huyse, and P. van Duppen, Phys. Rep. **215**, 101 (1992).
[55] P. Federman and S. Pittel, Phys. Lett. B **69**, 385 (1977).
[56] P. Federman and S. Pittel, Phys. Lett. B **77**, 29 (1978).
[57] P. Federman, S. Pittel, and R. Campos, Phys. Lett. B **82**, 9 (1979).
[58] P. Federman and S. Pittel, Phys. Rev. C **20**, 820 (1979).
[59] A. Petrovici, Phys. Rev. C **85**, 034337 (2012).
[60] R. A. Meyer, E. A. Henry, L. G. Mann, and K. Heyde, Phys. Lett. B **177**, 271 (1986).
[61] A. Kumar and M. R. Guyne, Phys. Rev. C **32**, 2116 (1985).
[62] J. Dobaczewski, in *Proceedings of the International Conference on Nuclear Structure Physics, Cocoyoc, Mexico, 1988*, edited by R. Casten, A. Frank, M. Moshinski, and S. Pittel (World Scientific, Singapore, 1988), pp. 227–242.
[63] J. Skalski, P.-H. Heenen, and P. Bonche, Nucl. Phys. A **559**, 221 (1993).
[64] W. Urban, T. Rząca-Urban, A. Złomaniec, G. Simpson, J. L. Durell, W. R. Phillips, A. G. Smith, B. J. Varley, I. Ahmad, and N. Schulz, Eur. Phys. J. A **16**, 11 (2003).
[65] T. R. Werner, J. Dobaczewski, M. W. Guidry, W. Nazarewicz, and J. A. Sheikh, Nucl. Phys. A **578**, 1 (1994).
[66] W. D. Kupl, J. L. Wood, K. S. Krane, J. Loats, P. Schmelzenbach, C. J. Stapels, R.-M. Larimer, and E. B. Norman, Phys. Rev. Lett. **91**, 102501 (2003).
[67] W. D. Kulp, J. L. Wood, P. E. Garrett, J. M. Allmond, D. Cline, A. B. Hayes, H. Hua, K. S. Krane, R.-M. Larimer, J. Loats, E. B. Norman, P. Schmelzenbach, C. J. Stapels, R. Teng, and C. Y. Wu, Phys. Rev. C **71**, 041303(R) (2005).
[68] W. Urban, J. A. Pinston, G. S. Simpson, A. G. Smith, J. F. Smith, T. Rzça-Urban, and I. Ahmad, Phys. Rev. C **80**, 037301 (2009).
[69] R. A. Meyer, E. Monnand, J. A. Pinston, F. Schussler, B. Pfeiffer, I. Ragnarsson, H. Lawin, G. Lhersonneau, and K. Sistemich, Nucl. Phys. A **439**, 510 (1985).
[70] J. K. Hwang, A. V. Ramayya, J. H. Hamilton, D. Fong, C. J. Beyer, P. M. Gore, Y. X. Luo, J. O. Rasmussen, S. C. Wu, I. Y. Lee, C. M. Folden, III, P. Fallon, P. Zielinski, K. E. Gregorich, A. O. Macchiavelli, M. A. Stoyer, S. J. Asztalos, T. N. Ginter, S. J. Zhu, J. D. Cole, G. M. Ter Akopian, Y. T. Oganessian, and R. Donangelo, Phys. Rev. C **67**, 054304 (2003).
[71] A. Złomaniec, H. Faust, J. Genevey, J. A. Pinston, T. Rząca-Urban, G. S. Simpson, I. Tsekhanovich, and W. Urban, Phys. Rev. C **72**, 067302 (2005).
[72] T. Rząca-Urban, W. Urban, M. Czerwiński, J. Wiśniewski, A. Blanc, H. Faust, M. Jentschel, P. Mutti, U. Köster, T. Soldner, G. de France, G. S. Simpson, and C. A. Ur, Phys. Rev. C **98**, 064315 (2018).
[73] K. Li, J. H. Hamilton, A. V. Ramayya, S. J. Zhu, Y. X. Luo, J. K. Hwang, C. Goodin, J. O. Rasmussen, G. M. Ter-Akopian, A. V. Daniel, I. Y. Lee, S. C. Wu, R. Donangelo, J. D. Cole, W. C. Ma, and M. A. Stoyer, Phys. Rev. C **78**, 044317 (2008).
[74] R. E. Azuma, G. L. Borchert, L. C. Carraz, P. G. Hansen, B. Jonson, S. Mattsson, O. B. Nielsen, G. Nyman, I. Ragnarsson, and H. L. Ravn, Phys. Lett. B **86**, 5 (1979).
[75] J. Skalski, S. Mizutori, and W. Nazarewicz, Nucl. Phys. A **617**, 282 (1997).
[76] P. Spagnoletti, G. Simpson, S. Kisyov, D. Bucurescu, J.-M. Régis, N. Saed-Samii, A. Blanc, M. Jentschel, U. Köster, P. Mutti, T. Soldner, G. de France, C. A. Ur, W. Urban, A. Astier, A. M. Bruce, C. Bernards, *et al.* (unpublished).
[77] J. A. Shannon, W. R. Phillips, J. L. Durell, B. J. Varley, W. Urban, C. J. Pearson, I. Ahmad, C. J. Lister, L. R. Morss, K. L. Nash, C. W. Williams, N. Schulz, E. Lubkiewicz, and M. Bentaleb, Phys. Lett. B **336**, 136 (1994).
[78] G. Gürdal and F. G. Kondev, Nucl. Data Sheets **113**, 1315 (2012).